

tance, it would seem, make FRP good candidates for prestressing bars. A problem is that FRP materials are very time and service dependent. Under steady load they show varying degrees of creep deformation: CFRP does not creep, GFRP shows a negligible creep, AFRP shows long-term deformations due to creep. In addition, fiberglass rods have premature rupture under sustained tensile load. Conducting constant voltage, a tensile strength of GFRP falls to values as low as 20% that causes rupture. Because of these reasons, the carbon fiber seems the most appropriate for FRP prestressing. Another problem that must be solved is the strengthening of rods. Special devices must be due to low strength in the transverse direction of the fibers. The advantage is that the FRP rods have a high tensile strength with moderate modulus and less sensitive to aging of concrete.

## REFERENCES

1. Di Ludovico, Marco. Experimental behavior of prestressed concrete beams with FRP / Di Ludovico, Marco. – Dipartimento di Analisi e Progettazione Strutturale, Anno Accademico, 2001–2002.
2. ASTM D3039/D 3039M-00. Standard Test Method for Tensile Properties of Polymer Matrix Composite Materials. American Standards of Testing and Materials.
3. Design recommendations for concrete structures prestressed with FRP tendos, FHWA CONTRACT.
4. DTFH61-96-C-00019, Final Report. – August, 1, 2001.
5. Burgoyne, C.J., (1988) Structural Applications of Parafil Rope, Symposium on Engineering Applications of Parafil Rope / C.J. Burgoyne. – Ed., Imperial College, London, 6 January. – P. 39–47.
6. Short-Term Sustained Loading of FRP Tendon-Anchorage Systems / A. Nanni [et al.] // Construction & Building Materials. – 1996. – Vol. 10, No. 4. – P. 255–266.

UDC 624.04=111

## CONSTRUCTION OF FLUIDITY BORDER TAKING INTO ACCOUNT PLASTIC ANISOTROPY

**ALEXANDER BOBROV, IGNATI ZAZERSKY, ALEXANDER SHCHERBO**  
**Polotsk State University, Belarus**

*Anisotropy due to plastic deformation was studied on tubular steel specimens. This type of anisotropy is found to influence the plastic strain increment vector as the stress point moves over the yield surface associated with a prescribed prestraining. The length of the plastic strain increment vector is found to decrease as the stress point moves from the point associated with the prestraining program. An appropriate measure of this effect is introduced in the form of a modulus of the effective plastic strain increment. Variation of the modulus over the yield surface is compared with the results furnished by the existing flow theories.*

Standard theories of plastic flow are formulated to calculate deformations along a given loading path only. Material anisotropy due to plastic deformation is either not accounted for, as it is the case in the theory of isotropic hardening, or is considered only as regards the change of shape and position of subsequent yield surfaces. In all such theories the following ratio:

$$K = -\frac{\delta\vartheta^P}{\delta S_{\delta\vartheta}}$$

Is assumed to be constant on each subsequent yield locus. This ratio - we shall call it the modulus of the effective plastic strain increment - involves  $\delta\vartheta^P$  which is the length of the plastic strain increment vector and  $\delta S_{\delta\vartheta}$ , which stands for projection of the stress increment vector on the direction of  $\delta\vartheta^P$ . According to this assumption all the vectors  $\delta S$  with equal  $\delta S_{\delta\vartheta}$  at any point of the yield surface which corresponds to an actually prestrained material produce the same  $\delta\vartheta^P$  [1].

The results of experiments [2, 3], suggest however, that the deformation induced anisotropy manifests itself not only through the change of shape and position of subsequent yield surfaces but also makes the modulus  $K$  to vary with the stress profile on these surfaces.

The aim of the present paper is to examine how the modulus (1) varies with the loading path and with stress trajectory on the yield surface.

The experiments have been carried out in plane stress under combined tension and torsion. A suitable experimental outfit has been developed, resembling that described in [4]. The deformations were measured by means of mirror extensometers.

Thin-walled, tubular specimens were manufactured from drawn mild steel tubes. The outer diameter and the wall thickness of the specimens were 12 mm and 0.5 mm respectively. Initial anisotropy was removed by annealing.

The test results were interpreted in stress and strain spaces referred to the coordinate systems:

$$S_1 = \sigma, S_2 = \tau\sqrt{3} \quad \text{and} \quad \vartheta_1^p = \varepsilon^p, \vartheta_2 = \gamma^p/\sqrt{3}.$$

The applied stresses are denoted by  $\sigma$  and  $\tau$  whereas  $\varepsilon^p$  and  $\gamma^p$  stand for plastic strains recorded in the program. The lengths of vectors  $S_i$  and  $\vartheta_i^p$  correspond to the equivalent stress and strain.

In order to establish the magnitude of the modulus  $K$  corresponding to the prescribed value of equivalent plastic strain, specimens without prior plastic prestraining were tested under proportional loading. For this purpose straight paths of loading associated with different values of the Lode parameter  $\mu$  were chosen and on each of such paths the magnitude of the modulus  $K$  was established at  $\vartheta_i^p$  equal to 3 per cent<sup>1)</sup>. Two specimens were tested for each loading path associated with a prescribed value of  $\mu$ .

The essential part of the testing procedure was as follows. After the specimens were subjected to equal initial plastic strain in tension or in torsion, they were unloaded and reloaded at different angles to the direction of prestraining well into the plastic range.

<sup>1)</sup> The material used had a long platform of yielding. Such an extensive deformation was necessary in order to ensure entering into the hardening range.

Values of the modulus  $K$  were determined for each loading path when the yield surface associated with the prestraining was reached and plastic strains were evaluated by subtracting elastic strains from the measured strains by disregarding variations in the elastic moduli  $E$  and  $G$  with plastic deformation. In order to eliminate the influence of viscous effects, specimens were loaded in steps of  $\delta S_i = 100 \text{ kg/cm}^2$  with an adequate time interval between the consecutive steps. The results are presented in Figs. 1 and 2 where the abscissa specifies the angle  $\alpha$  between the initial and the consecutive path of loading and the ordinate represents the ratio  $\eta = K_a/K_0$ .  $K_0$  denotes the modulus of plastic strain increment at the end of prestraining and  $K_a$  the corresponding value for the second loading. The magnitudes of initial plastic strain are marked on the corresponding curves.

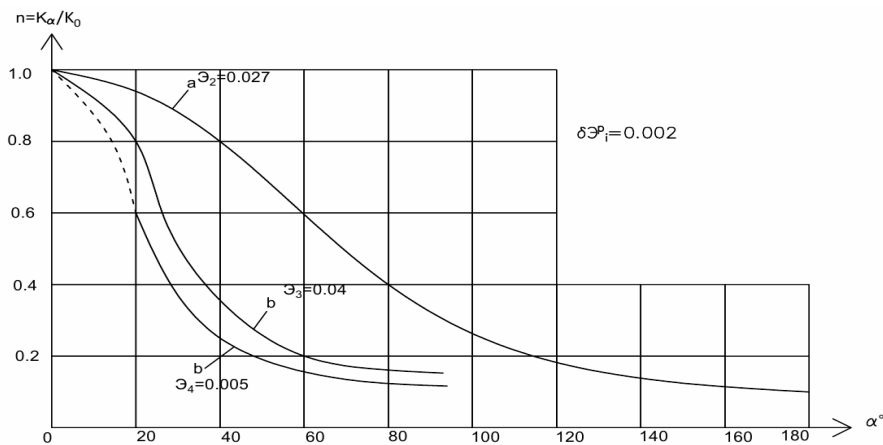


Fig. 1. Variation of the modulus K along the yield curve. Steel specimens,  $\delta\vartheta_i^p=0.002$

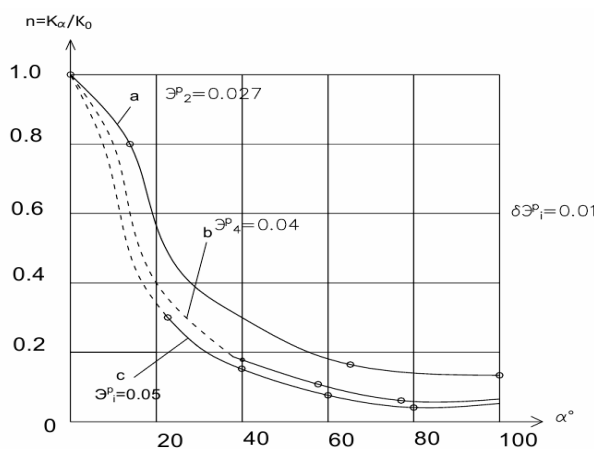


Fig. 2. Variation of the modulus K along the yield curve. Steel specimens  $\delta\vartheta_i^p=0.01$

Fig. 1 specifies the variation of  $K$  along the yield curve. The value of plastic strain increment at which  $K$  defined in (1) was computed is  $\vartheta_i^p=0,002$ . Similar curves relating to  $\vartheta_i^p = 0.001$  are plotted in Fig. 2. In these

figures the lines labelled a) correspond with results of specimens prestrained in torsion whereas those marked b) and c) represent results of specimen exposed to initial deformation in tension. Every experimental point marked in the figures is the average value taken from two specimens. The figures show that the modulus  $K$  decreases significantly with  $\alpha$  along the yield curve, i.e. with the distance from the stress point associated with prestraining.

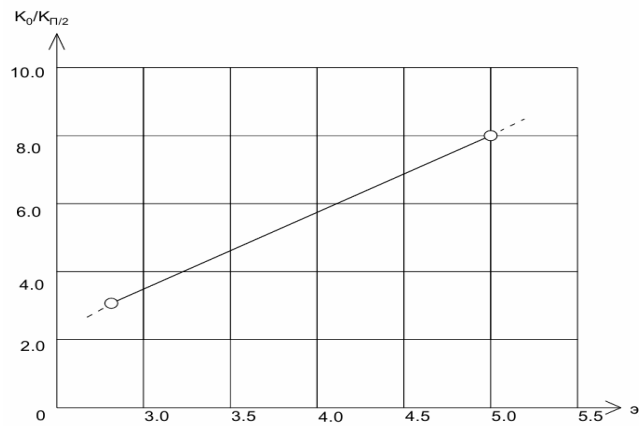


Fig. 3. Rate of change of the modulus  $K$  along the yield curve depending on the value of initial plastic strain

It can be seen in Figs. 1 and 2 that the effective range of prestraining increases with both, the magnitude of initial plastic deformation and a reduction in the offset used when specifying the yield curve. The extent of the change in  $K$  along the yield curve may partly be characterized by the ratio  $K_0/K_{\pi/2}$ , where  $K_{\pi/2}$  is the modulus corresponding to the stress point specified by the radius-vector which makes the angle  $\alpha = \pi/2$  with the direction of prestraining. In Fig. 3 the plot of  $K_0/K_{\pi/2}$  against initial effective plastic strain is given. It can be readily seen that this relationship is well approximated by a straight line for a comparatively narrow range of initial strains considered in the experiments.

Variation of the modulus  $K$  with the length of the stress profile on the yield curve and with the length of the secondary loading path

$\Delta S_i \backslash \alpha$	0	150	300	450	600
0°	3.7*0,001	4.3*0,001	5.0*0,001	6.4*0,001	8.6*0,001
25°	3.2*0,001	3.8*0,001	4.4*0,001	5.5*0,001	6.4*0,001
65°	2.2*0,001	3.1*0,001	4.0*0,001	5.0*0,001	6.2*0,001
90°	1.2*0,001	2.2*0,001	3.2*0,001	4.3*0,001	5.3*0,001
130°	5.2*0,0001	6.0*0,0001	8.0*0,0001	1.2*0,001	1.8*0,001
180°	3.5*0,0001	4.1*0,0001	6.0*0,0001	7.0*0,0001	1.0*0,001

$\Delta S_i \backslash \alpha$	750	850	950	1050	1150	1250
0°						
25°	7.9*0,001					
65°	7.6*0,001	9.1*0,001				
90°	6.6*0,001	7.5*0,001	8.5*0,001			
130°	2.4*0,001	3.2*0,001	3.9*0,001	4.6*0,001	5.6*0,001	7.2*0,001
180°	1.5*0,001	1.8*0,001	2.2*0,001	2.7*0,001	3.1*0,001	3.7*0,001

In order to eliminate a possible conjecture that the observed variation of the modulus  $K$  is a property of the steel tested, similar experiments were conducted on nickel tubes (outer diameter 5 mm, wall thickness 0.2 mm). The specimens were subjected to initial plastic prestraining of 0.011 and variations of  $K$  were recorded along the yield curve corresponding to an offset of 0.0002. These results are represented in Fig. 4, but cannot be compared quantitatively with the curves shown in Figs. 1 and 2. However, it may be concluded that changes along yield curves in the modulus  $K$  introduced in this work prove to be a common property of metals.

As already mentioned, the modulus  $K$  was measured for the secondary straight paths of loading along the yield curve established by using a standard offset of 0.002. A certain regularity of change in  $K$  was observed which appears to depend on how far secondary paths of loading  $\Delta S_i$  advanced into the plastic range. It was found that at increasing  $\Delta S_{i0}$  the difference between the  $K$ 's for different paths of secondary loading decreased and vanished at a definite value  $\Delta S_{i0}$  at which the magnitudes of the modulus reached the stable value  $K_0$ . The quantity  $\Delta S_{i0}$  is called 'the length of restoration path of  $K$ ' and should not be confused with the so called trace of delay of scalar properties. Loci corresponding to stationary values of  $K$  are called 'isomodular lines'.

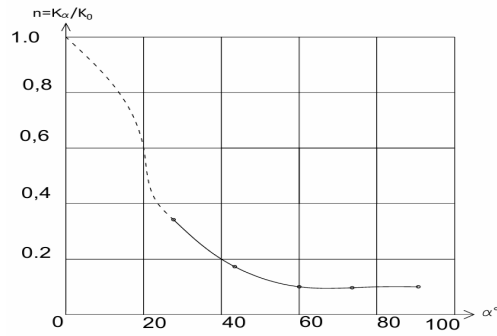


Fig. 4. Variation of the modulus K along the yield curve.  
Nickel specimens  $\delta\mathcal{E}_i^p=0.02$

In Figs. 5-7 the yield curves obtained using the standard offset of 0.002 (curves a) and the corresponding isomodular lines (curves b) are presented for specimens subjected to plastic prestrain of 0.02,0.07, 0.04 and 0.05 4 respectively. In Fig. 5 the results of the most complete analysis of the curves are represented. The specimens of the relevant experiment were subjected to plastic prestraining in torsion, and the angles of secondary loading paths were  $0 \leq \alpha \leq \pi$ . The shaded area of the diagram corresponds to the states associated with 'slight' plastic strains, i.e. to the restoration path of K. Numerical values of K are given in mm<sup>2</sup>/kg on table 1. On the basis of both the tabulated data and the curves presented in Fig. 5 it is evident that the length  $\Delta S_{i0}$  of the restoration path of K depends on the angle  $\alpha$  defined before the length increases as the angle grows. In Figs. 6 and 7 the curves corresponding to the specimens subjected to prestraining in tension are given. The curves are shown only in the first quadrant of the  $\{S_1, S_2\}$  plane. It is easy to see that in these cases also  $\Delta S_{i0}$  increases as  $\alpha$  grows. The comparison of the curves presented in figures leads to the conclusion that the restoration path length  $\Delta S_{i0}$  of the modulus depends also on the value of initial plastic strain.

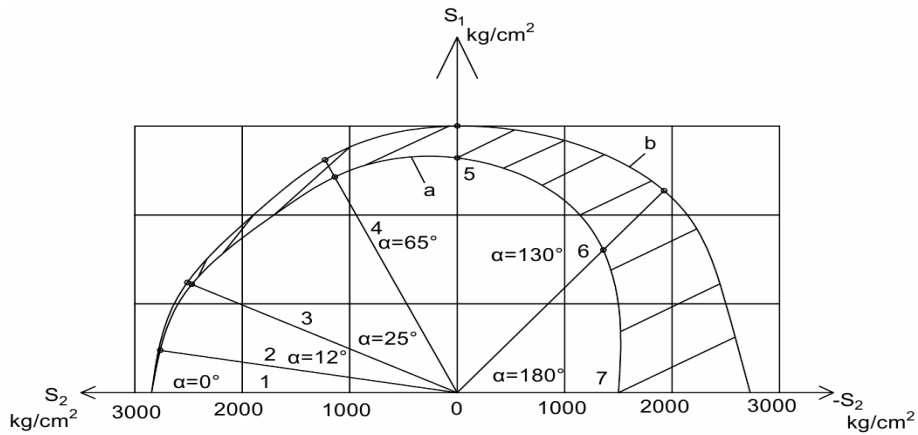


Fig. 5. Yield curve and isomodular line for specimens subjected to plastic prestraining in torsion, at 0.027 of equivalent strain

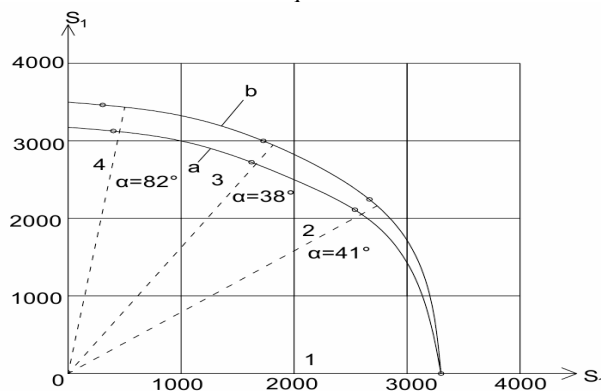


Fig. 6. Yield curve and isomodular line for specimens subjected to plastic prestraining in tension, at  $\mathcal{E}_i^p=0.04$

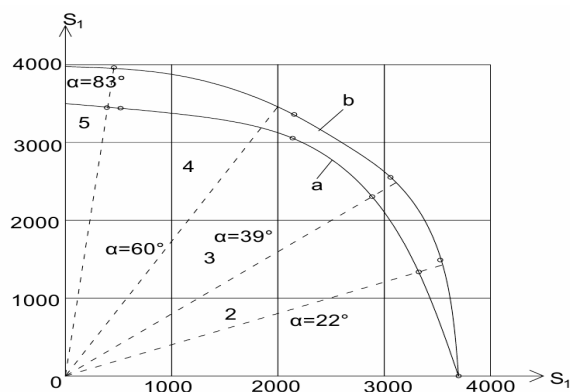


Fig. 7. Yield curve and isomodular line for specimens subjected to plastic prestraining in tension, at  $\varepsilon^p=0.05$

In order to estimate errors that are caused by neglecting the anisotropy considered in the paper, experimental data and theoretical predictions obtained by the theory of kinematical hardening and by the theory accounting for the Bauschinger effect were compared, by considering and disregarding a change of modulus  $K$ . The comparison was made for two combined loading paths which caused the greatest discrepancy between theoretical results and experimental data.

Plastic strain components were determined in graphic form using the curve  $\sigma - \varepsilon^p$  obtained experimentally from data of tensile specimens. The results are presented in Figs. 1-7. The effect of the variable  $K$  on the accuracy of analytical predictions is most pronounced in Fig. 5, in which plastic strains found experimentally and evaluated theoretically by accounting for the Bauschinger effect are compared for a specimen subjected to initial shearing strain  $\varepsilon^p = 2.7$  per cent.

The strain components obtained in accordance with the mentioned theories even allowing for the described plastic strain induced anisotropy, deviate considerably from those found experimentally (this applies specifically to the theory of kinematical hardening). No better agreement can, however, be expected as we take into account, only one of the factors influencing inaccuracy of the available flow theories. And in view of some reasons for this inaccuracy of the flow theories can be given, i.e. lack of coincidence of the yield loci obtained experimentally and theoretically. Also the influence of the stress deviator on the plastic deformation process was not considered in any of the mentioned theories. The accuracy of these theories is also influenced by the fact that the deviators of stress and plastic strain are not coaxial even under proportional loading as found by several investigators.

#### REFERENCES

1. Prager, W. The theory of plasticity: a survey of recent achievements. James Clayton Lecture, Proceed, of the Inst, of Mech. Eng., (1955).
2. Yougn, Y.I. and O. A. Shishmarev, Dokl. Akad. Nauk S.S.S.R. – 1958. – 119. – 468.
3. Isotov, I.N. and Y. I. Yougn, Dokl Akad. Nauk S.S.S.R. – 1961. – 139. – 576–579.
4. Yougn, Y.I. and O. A. Shishmarev, Zavodskaya Laboratoriya. – 1958. – 10. – 1243–1245.

UDC 624.072

### STRAIN CALCULATION FOR COMPRESSED CURVED BAR UNDER COMBINED APPLICATION OF THERMAL EXPOSURE AND LOAD

EVGENIYA VOLKOVA, LEONID TURISHCHEV  
Polotsk State University, Belarus

*Differential equation of the axis of a compressed curved bar with unspecified ends fixity under combined application of thermal exposure and load has been obtained. Application of the obtained equation for strain calculation for a beam, hinged at its ends, has been demonstrated.*

It is usual practice to carry out analysis of structures in relation to load exposure and temperature exposure separately and subsequently summate the determined stress-strain state (SSS) parameters in accordance with the principle of superposition. But this approach is true for linearly strained structures only. In case of flexible structures geometrical nonlinearity and structure strain calculation must be taken into account. Such issues as